



HAL
open science

Developmental atlas of white lupin cluster roots

Cecilia Gallardo, Barbara Hufnagel, Alexandre Soriano, Fanchon Divol,
Laurence Marquès, Patrick Doumas, Benjamin Peret

► **To cite this version:**

Cecilia Gallardo, Barbara Hufnagel, Alexandre Soriano, Fanchon Divol, Laurence Marquès, et al..
Developmental atlas of white lupin cluster roots. 2020. hal-02527454

HAL Id: hal-02527454

<https://hal.science/hal-02527454>

Preprint submitted on 1 Apr 2020

HAL is a multi-disciplinary open access archive for the deposit and dissemination of scientific research documents, whether they are published or not. The documents may come from teaching and research institutions in France or abroad, or from public or private research centers.

L'archive ouverte pluridisciplinaire **HAL**, est destinée au dépôt et à la diffusion de documents scientifiques de niveau recherche, publiés ou non, émanant des établissements d'enseignement et de recherche français ou étrangers, des laboratoires publics ou privés.



Distributed under a Creative Commons Attribution - NonCommercial - NoDerivatives 4.0
International License

1 **Developmental atlas of white lupin cluster roots**

2

3 Cécilia Gallardo, Bárbara Hufnagel, Alexandre Soriano, Fanchon Divol, Laurence Marquès,

4 Patrick Doumas and Benjamin Péret*

5

6 BPMP, Univ Montpellier, CNRS, INRAE, Institut Agro, Montpellier, France

7

8 **Correspondence**

9 *Corresponding author,

10 tel : (+33)499612859

11 e-mail : benjamin.peret@cnrs.fr

12

13 Date of submission: **25th March 2020**

14 Number of figures: **8**

15 Number of tables: **1**

16 Word count: **4502**

17

18

19

20

21

22

23

24

25

26

27

28

29

30

31

32

33

34

35 **Running title**

36 Developmental atlas of white lupin cluster roots

37

38 **Highlight**

39 White lupin cluster roots consist in the formation of numerous rootlets whose development
40 can be divided in 8 stages and involves divisions in the pericycle, endodermis and cortex.

41

42 **Abstract**

43 During the course of evolution, plants have developed various strategies to improve
44 micronutrient acquisition, such as cluster roots. These spectacular structures are dedicated to
45 efficient phosphate remobilization and acquisition. When exposed to Pi-limitation, white
46 lupin forms cluster roots made of dense clusters of short specialized roots, called rootlets.
47 Although the physiological activity of rootlets has been well studied, their development
48 remains poorly described. Here, we provide a developmental atlas of white lupin early rootlet
49 development, using molecular markers derived from the model plant *Arabidopsis*. We first
50 focused on cell division patterns to determine which cells contribute to the rootlet
51 primordium. Then, we identified homologs of previously described tissue specific genes
52 based on protein sequence analysis and also using detailed transcriptomic data covering
53 rootlet development. This study provides a comprehensive description of the developmental
54 phases of rootlet formation, highlighting that rootlet primordium arises from divisions in
55 pericycle, endodermis and cortex. We describe that rootlet primordium patterning follows
56 eight stages during which tissue differentiation is established progressively.

57

58 **Keywords (6-10)**

59 White lupin, cluster roots, rootlets, root development, patterning, primordium, phosphate.

60

61 **Introduction**

62 Cluster roots (CRs) are considered to be one of the major adaptations to improve plant
63 nutrient acquisition, together with nitrogen-fixing nodules and mycorrhizae (Neumann and
64 Martinoia, 2002). However, CRs differ from nodules and mycorrhizae as they form without
65 the presence of a symbiotic partner (Lamont, 2003). CR bearing species can be found in soils
66 where nutrients are poorly available (Dinkelaker *et al.*, 1995; Lambers *et al.*, 2003). Plants
67 forming CRs can absorb inorganic phosphate (Pi) at a faster rate than non-forming CRs plants
68 and access to a larger pool of Pi due to increased soil exploration (Vorster and Jooste, 1986).

69 Because this developmental adaptation has a selective advantage, CR arose in a whole range
70 of distant families from Cyperaceae and Restionaceae in monocots to Betulaceae,
71 Casuarinaceae, Cucurbitaceae, Eleagnaceae, Fabaceae, Moraceae, Myricaceae and Proteaceae
72 in dicots (Dinkelaker *et al.*, 1995; Lambers *et al.*, 2003). Interestingly, most of these families
73 have lost the ability to form mycorrhizae (Oba *et al.*, 2001; Delaux *et al.*, 2014; Maherali *et*
74 *al.*, 2016).

75 CR is an adaptive trait of plants to cope with P-depleted soils (Neumann and Martinoia, 2002;
76 Lambers *et al.*, 2015). Because phosphate is mostly concentrated in the topsoil layer, CRs are
77 mainly produced in the upper part of the root system (Lynch and Brown, 2001). Hereafter,
78 CRs will refer to the entire length of the lateral root that comprises at least one cluster of
79 tightly grouped third-order roots termed rootlets (Dinkelaker *et al.*, 1995; Skene, 1998). CRs
80 are an exacerbated developmental response that results from massive induction of rootlets and
81 represent a good model to study root adaptive developmental responses to abiotic constraints.
82 White lupin (*Lupinus albus*) is one of only few crops that can form CRs (Fig. 1A-C). It has
83 received most attention for studies on CR morphology and physiology (Johnson *et al.*, 1996;
84 Watt and Evans, 1999; Hagström *et al.*, 2001; Neumann and Martinoia, 2002; Uhde-Stone *et*
85 *al.*, 2003; Cheng *et al.*, 2011). White lupin (WL) can form up to 35-45 rootlets per cm
86 (Dinkelaker *et al.*, 1989) and secrete massive amount of organic acids and protons
87 (Massonneau *et al.*, 2001; Sas *et al.*, 2001; Neumann and Martinoia, 2002). Such
88 physiological modifications can increase the Pi availability of soil, resulting in a beneficial
89 effect to other species in mixed cultures (Braum and Helmke, 1995; Cu *et al.*, 2005; Li *et al.*,
90 2010). For instance, mixed culture of wheat and white lupin was shown to increase shoot Pi
91 uptake up to 45 % in wheat (Cu *et al.*, 2005). This shows how white lupin can be used to
92 improve the poor efficiency of Pi uptake by several crops for a sustainable agriculture
93 perspective.

94 In many angiosperms, secondary roots (or lateral roots) arise from pericycle as described in
95 the model plant *Arabidopsis thaliana* (Laskowski *et al.*, 1995; Malamy and Benfey, 1997;
96 Orman-Ligeza *et al.*, 2013; Herrbach *et al.*, 2014). In some monocots, lateral roots show
97 contribution of dividing endodermal cells including some Poaceae like rice (*Oriza sativa*) and
98 maize (*Zea mays*) (Hochholdinger *et al.*, 2004). In dicots, some Legume species also show
99 contribution of division in endodermis and cortex including soybean (*Glycine max*), *Lotus*
100 *japonicus* and alfalfa (*Medicago truncatula*) (Byrne *et al.*, 1977; Op den Camp *et al.*, 2011;
101 Herrbach *et al.*, 2014). In *Arabidopsis*, it was proposed that lateral root primordium
102 development proceeds through an 8-stage process (Malamy and Benfey, 1997) that can be

103 summed up as a two-step developmental model (Laskowski *et al.*, 1995). Early
104 developmental phase of lateral root primordium (stage I-IV) starts with the first division in
105 two adjacent pericycle cells followed by several rounds of divisions to produce a four-layered
106 primordium (Malamy and Benfey, 1997). Then, cells start to differentiate and acquire various
107 identities as tissues organize around a meristematic zone (stage V-VII) (Trinh *et al.*, 2018).
108 Transition between these two developmental phases marks the onset of quiescent centre
109 establishment and formation of meristematic initials (Goh *et al.*, 2016). With regards to these
110 processes, very little information is available for third-order roots, both in Arabidopsis and
111 lupin. In WL, it was described that xylem pole pericycle cells are recruited to become founder
112 cells (Johnson *et al.*, 1996) and a predominant role for auxin was demonstrated (Gallardo *et*
113 *al.*, 2019). However, a full description of the entire developmental process of rootlet
114 formation is still missing.

115 In an effort to generate a developmental atlas of rootlet formation in white lupin, we
116 performed an anatomic study to define discrete developmental stages throughout early rootlet
117 development. Since the root structure of WL is more complex than Arabidopsis root, it
118 appeared important to use a set of various molecular markers to identify division and
119 differentiation events. We first used the cell division marker *CYCLIN B1;1* (*CYCB1;1*) from
120 Arabidopsis whose promoter revealed to drive expression in WL dividing cells. This allowed
121 us to identify cell division in pericycle but also in endodermal and cortical cells during rootlet
122 formation. In a second approach, we decided to take advantage of a set of tissular markers and
123 identify their homolog genes in WL genome. We combined sequence analysis to detailed
124 expression profiling to select the best candidates amongst WL highly duplicated gene
125 families. We generated transgenic hairy root plants expressing these tissular markers that
126 show a strong conservation of tissular specificity. Using this approach, we provide a
127 developmental atlas of cell division and differentiation during white lupin rootlet primordium
128 development.

129

130 **Materials and methods**

131 *Plant materials and growth conditions*

132 Seeds of white lupin (*Lupinus albus* L. cv. *Amiga*) calibrated at 7 mm were used in all
133 experiments. White lupin plants were cultivated in growth chambers under controlled
134 conditions (16 h light / 8 h dark, 25°C day / 20°C night, 65 % relative humidity, and PAR
135 intensity 200 $\mu\text{mol}\cdot\text{m}^{-2}\cdot\text{s}^{-1}$) in hydroponic conditions. The hydroponic solution was modified
136 from (Abdolzadeh *et al.*, 2010) without phosphate, and was composed of: MgSO_4 54 μM ;

137 Ca(NO₃)₂ 400 μM; K₂SO₄ 200 μM; Na-Fe-EDTA 10 μM; H₃BO₃ 2.4 μM; MnSO₄ 0.24 μM;
138 ZnSO₄ 0.1 μM; CuSO₄ 0.018 μM; Na₂MoO₄ 0.03 μM. Plants were grown either in 1,6 L pots
139 or 200 L tanks. Solution was aerated continuously. For plants in pots, the nutrient solution
140 was renewed every 7 days.

141

142 *Molecular cloning*

143 The primers to amplify the promoter sequences of *LaSCR1*, *LaWOL*, *LaPEP*, *LaEXP7* were
144 designed using Primer3plus ([http://www.bioinformatics.nl/cgi-](http://www.bioinformatics.nl/cgi-bin/primer3plus/primer3plus.cgi)
145 [bin/primer3plus/primer3plus.cgi](http://www.bioinformatics.nl/cgi-bin/primer3plus/primer3plus.cgi)). All primer sequences used are summarized in Table S1.
146 Primers were used to amplify at the minimum 1500 bp upstream of the start codon from white
147 lupin genomic DNA. Sizes of all the promoters amplified are summarized in Table S1. AttB1
148 (5'-GGGGCCAAGTTTGTACAAAAAAGCAGGCT-3') and attb2 (5'-
149 CCCCCCACTTTGTACAAGAAAGCTGGGT-3') adapters were added to the primers.
150 Amplified fragments were subsequently cloned into the pDONR221 by Gateway reaction.
151 The promoters were then cloned into the binary plasmid pKGWFS7 containing a GFP-GUS
152 fusion by Gateway cloning.

153

154 *Bacterial strain*

155 *Agrobacterium rhizogenes* strain *ARqual* was used to perform *hairy root* transformation of
156 white lupin. Bacteria were transformed with the binary plasmid by electroporation.
157 Transformation was confirmed by PCR and sequencing. LB agar plates added with sucrose
158 2%, acetosyringone 100 μM and appropriate antibiotics were inoculated with 200 μL of liquid
159 bacteria culture, and incubated at 28°C for 24 h to get a bacterial lawn. Bacterial lawn was
160 used for white lupin seedling transformation.

161

162 *Hairy root transformation of white lupin*

163 White lupin hairy root transformation was performed as previously described (Uhde-Stone *et*
164 *al.*, 2005). White lupin seeds caliber 8 mm were surface sterilized by 4 washes in osmosis
165 water, 30 min sterilization in bleach (Halonet 20%) and washed 6 times in sterile water under
166 sterile conditions. Seed were germinated on half MS medium (pH was adjusted to 5.7). After
167 germination, radicles of 1 cm were cut over 0.5 cm with a sterile scalpel. The radicles were
168 inoculated with the *Agrobacterium rhizogenes* lawn. Fifteen inoculated seedlings were placed
169 on square agar plates (0.7 % agar in 1X Hoagland solution) containing 15 μg.mL⁻¹
170 Kanamycin. Composition of Hoagland medium without phosphate was the following one:

171 MgSO₄ 200 μM; Ca(NO₃)₂ 400 μM; KNO₃ 325 μM; NH₄Cl 100 μM; Na-Fe- EDTA 10 μM;
172 H₃BO₃ 9.3 μM; MnCl₂ 1.8 μM; ZnSO₄ 0.17 μM; CuSO₄ 0.06 μM; Na₂MoO₄ 2.3 μM. Plates
173 were placed vertically in controlled conditions: 16 h light / 8 h dark, 25°C day / 20°C night,
174 65 % relative humidity, and PAR intensity 200 μmol.m⁻².s⁻¹. After 7 days on plates, 60
175 seedlings were transferred to 12x16.5x5.5 cm trays (20 seedlings per tray) and watered with
176 500 mL pure water. After 12 days, plants presenting hairy roots were transferred to
177 hydroponics in 1.6 L pots containing nutrient solution. Nutrient medium was renewed each
178 week. After 7 days in hydroponic conditions, CRs were sampled on *hairy root* plants.

179

180 *Histochemical analysis*

181 Histochemical staining of β-glucuronidase was performed on CRs from *hairy root* plants.
182 Samples were incubated in a phosphate buffer containing 1 mg.mL⁻¹ X-gluc as a substrate (X-
183 Gluc 0.1 %; phosphate buffer 50 mM, pH 7, potassium ferricyanide 2 mM, potassium
184 ferrocyanide 2 mM, Triton X-100 0.05 %). Zone of CRs with non-emerged rootlets were
185 cutted into 4 to 5 sections and fixed (formaldehyde 2%, glutaraldehyde 1%, caffeine solution
186 1%, phosphate buffer at pH 7). Fixation was performed for 2.5 h under agitation at room
187 temperature and then 1.5 h at 4°C.

188

189 *Microscopy analysis*

190 To generate thin sections, roots were progressively dehydrated in ethanol solutions with
191 increased concentrations: 50% (30 min), 70% (30 min), 90% (1 h), 95% (1 h), 100% (1 h),
192 100% (overnight). Samples were impregnated with 50% pure ethanol and 50% resin (v/v) for
193 2 days, then in 100 % resin for 5 days. CRs were embedded in Technovit 7100 resin (Heraeus
194 Kulze, Wehrheim, Germany) according to the manufacturer's recommendations. Thin
195 sections of 10 μm were produced using a microtome (RM2165, Leica Microsystems) and
196 counterstained for 30 min with 0.1% ruthenium red and rinsed two times with ultrapure water.
197 For nuclei visualization, 10 μm thick cluster roots sections were stained for 10 min with 3 μM
198 DAPI solution in PBS buffer at room temperature. After washing root three times with PBS
199 buffer for 5 min, the section were mounted in PBS buffer and analyzed. An argon laser at 405
200 nm provided excitation for DAPI staining. The fluorescence emission signal was detected
201 using a band-pass filter of 420-480 nm for DAPI. Imaging was performed in Montpellier RIO
202 imaging Platform (<http://www.mri.cnrs.fr/fr/>) with a stereomicroscope (SZX16, Olympus) for
203 macroscopic root images, an epifluorescence microscope with a colour camera (Olympus
204 BX61 with Camera ProgRes[®]C5 Jenoptik and controlled by ProgRes Capture software) for

205 thin root section, and a confocal microscope (Leica SP8, Leica Microsystems,
206 <https://www.leica-microsystems.com/fr/>) for nuclei visualization.

207

208 *Phylogenetic trees*

209 White lupin cDNA-deduced protein sequences were retrieved from the available white lupin
210 genome sequence tool (<https://www.whitelupin.fr/>). Arabidopsis protein sequences were
211 extracted from TAIR database (<https://www.arabidopsis.org>) and protein sequences from
212 *Lupinus angustifolius*, *Medicago truncatula*, *Cicer arietinum*, *Glycine max* were downloaded
213 from NCBI database (<https://www.ncbi.nlm.nih.gov/guide/proteins/>). Phylogenetic trees were
214 constructed using the phylogeny tool NGPhylogeny.fr (<https://ngphylogeny.fr/>) (Lemoine *et*
215 *al.*, 2019). The bootstrap consensus tree was inferred from 500 replicates. Branches
216 corresponding to partitions reproduced in less than 50% bootstrap replicates were collapsed.
217 Sequences were aligned using MUSCLE 3.7 and Gblocks with default parameters were used
218 to eliminate poorly aligned positions and divergent regions. PhyML 3.0 was used to perform
219 phylogenetic inference, using SH-like as aLRT test. Tree visualization was performed through
220 the iTOL v4.4.2 platform (Letunic and Bork, 2019).

221

222 **Results**

223

224 *Describing the developmental stages of rootlet primordium*

225 To provide a detailed description of cluster root development, thin longitudinal sections of 7
226 to 9 day-old lupin seedlings were stained with ruthenium red to observe all developmental
227 stages. Early events of rootlet development could be described in 8 discrete developmental
228 stages (Fig. 1D).

229 **Stage I.** Initiation is the first visible event of CR formation. It consists of two asymmetrical
230 anticlinal divisions in the pericycle (Fig. 1D StIa). Initiation continues with the appearance of
231 divisions in parallel orientation compared to the root axis (Fig. 1D StIb, black arrow). In the
232 longitudinal plane, close to 6 cells show these periclinal divisions. Peripheral cells are not
233 dividing, creating the boundaries of the primordium. In the overlaying endodermis, an
234 increased number of anticlinal divisions is clearly seen as compared to the surrounding
235 endodermal cells. About 8 cells are formed from these divisions.

236 **Stage II.** All pericycle cells participating in the rootlet primordium seem to have divided.
237 These divisions in the pericycle lead to the formation of two layers, named P1 (inner layer)
238 and P2 (outer layer). Following these divisions, cells start to swell and expand in the radial

239 direction. Simultaneously, periclinal divisions occur in the endodermis that divides this layer
240 into E1 (inner layer) and E2 (outer layer) (Fig. 1D StII, black arrow).

241 **Stage III.** A dozen of cells continue to divide in the 4-layered primordium. Anticlinal
242 divisions are seen in the most peripheral cells in the endodermis. At the same time, anticlinal
243 divisions are also seen in the cortex (Fig. 1D StIII, purple arrows).

244 **Stage IV.** A typical dome shaped rootlet primordium begins to form. The dividing cortex
245 comprises 10 cells in length. Four cells at the base of the primordium started to divide
246 between the xylem pole and the P1 inner layer (Fig. 1D StIV, black arrow) giving rise to the
247 future vasculature. Numerous radial, anticlinal and periclinal divisions happen in the tissues
248 derived from pericycle, endodermis and cortex.

249 **Stage V.** Primordium expands radially, pushing the overlaying cortical layers. Cells at the
250 base of the primordium (Fig. 1D StV, black arrow) continue to divide. The number of cells in
251 the overlaying cortex increases to 11 cells in length and are now forming part of the tip of the
252 primordium.

253 **Stage VI.** The rootlet primordium is now strongly deforming the cortical layers around. The
254 stage VI primordium begins to look like a mature root with several layers, although a typical
255 meristematic organization is not clear yet due to the apparent absence of a quiescent centre. In
256 the absence of tissue-specific markers, it is difficult to make strong assumption regarding the
257 nature of each tissue. The presence of elongated cells at the base of the primordium seems to
258 indicate the onset of the vasculature.

259 **Stage VII.** The rootlet primordium is about to cross the last layer of the cluster root, the
260 epidermis. As the primordium enlarges, distinguishing the different tissues inside the growing
261 rootlet becomes challenging due to the high number of cells. Many anticlinal divisions seem
262 to continue in the different layers of the primordium. The vascular tissue seems to be now
263 fully established as many elongated cells are connecting the cluster root stele to the rootlet
264 primordium.

265 **Stage VIII.** No visible difference can be seen in the cellular organization of the primordium
266 but cell elongation pushes the primordium beyond the epidermis and the primordium reaches
267 the rhizosphere.

268

269 *Following cell divisions during rootlet primordium formation*

270 Although many cell divisions can be seen from cell shape and the appearance of extra
271 division planes, the use of a molecular division marker allows to easily monitor mitotic
272 activity and define dividing cells at an early stage. The promoter of the *Arabidopsis thaliana*

273 *CYCBI;1* gene is activated during the G2/M transition (Colón-Carmona *et al.*, 1999). We
274 transformed WL roots with a construct containing the Arabidopsis *CYCBI;1* promoter fused
275 to the β -glucuronidase reporter gene (pAt*CYCBI;1::GUS*). This marker shows expression in
276 the cluster root apex, very similar to the expression described in Arabidopsis, suggesting a
277 conservation of the expression during cell cycle (Supplementary Figure S1A). Similarly,
278 expression is visible at early stages of rootlet initiation and throughout the developmental
279 process up to their emergence (Supplementary Figure S1B-D). We next produced thin cross
280 sections to analyse in detail the mitotic activity in cells of the rootlet primordia. We observed
281 that the first visible event of rootlet initiation is the activation of the pAt*CYCBI;1::GUS*
282 marker in one pericycle cell in front of each xylem pole (Fig. 2A), before division is visible
283 from an anatomical point of view, defining Stage 0. Subsequently, one or more divisions are
284 seen in the pericycle cells (Fig. 2B,C) suggesting that more than one cell participate in the
285 creation of the primordium. Then, divisions are also seen in the endodermis (Fig. 2C) and
286 cortex (Fig. 2D). These divisions seem mainly periclinal and therefore produce extra layers of
287 these tissues. Once the rootlet primordium reaches emergence, several divisions can be seen
288 in what seems to be a fully dividing meristematic zone (Fig. 2E).

289

290 *Expression of tissue-specific markers in CR*

291 Classic histology allows to describe precisely the early developmental stages of rootlet
292 formation and to define discrete stages associated with particular anatomic features. However,
293 cell types cannot be easily identified based solely on their shape during early developmental
294 stages. To which extent pericycle, endodermis and cortex tissues are involved in rootlet
295 initiation and rootlet outgrowth has yet to be determined. Another matter is to determine when
296 tissues are starting to differentiate. To address these questions, a limited number of molecular
297 markers (using the β -glucuronidase gene as reporter) specifically expressed in different tissue
298 types were tested. The corresponding white lupin genes were chosen (1) based on the protein
299 sequence homology between known molecular markers in the model plant *Arabidopsis*
300 *thaliana* and (2) based on their expression profile in the white lupin transcriptomic dataset.
301 Due to genome triplication, gene families are often larger in white lupin than in Arabidopsis
302 (Hufnagel *et al.*, 2020) and expression data helped directing our choice.

303 First, we chose a list of molecular markers based on their tissular expression in *Arabidopsis*
304 *thaliana*: two endodermal markers (WOL, SCR1), one cortical markers (PEP) and one
305 epidermal marker (EXP7) (Sbabou *et al.*, 2010; Marquès-Bueno *et al.*, 2016; Sevin-Pujol
306 *et al.*, 2017). Orthologous lupin genes were found by comparing Arabidopsis protein sequences

307 with all the cDNA-deduced protein sequences of WL genome. Comparison was made by
308 multiple comparison alignment by local BLAST on the white lupin database and by
309 generating phylogenetic trees containing the Arabidopsis sequence as well as Legume
310 relatives: *Medicago truncatula*, *Cicer arietinum*, *Lupinus angustifolius* and *Glycine max* (Fig.
311 3). On the other hand, expression profiles of the selected WL genes were checked in a
312 transcriptomic RNAseq database describing the spatial portions of a 5 days-old cluster root
313 and therefore covering the different developmental stages from S0 to S7 (Fig. 4A) (Hufnagel
314 *et al.*, 2020). All genes were found to be expressed during rootlet development and genes
315 were discriminated on their level of expression. For each gene family (3 to 4 genes), one gene
316 was found to be more highly expressed than the others and was selected assuming that high
317 gene expression would translate into a nicely visible marker (Fig. 4B-D). As a result, we
318 selected the following WL genes for further analysis: *Lalb_Chr04g0258751* (WOL),
319 *Lalb_Chr19g0123861* (SCR1), *Lalb_Chr11g0065071* (PEP) and *Lalb_Chr09g0324651*
320 (EXP7). Gene sequence and expression data can be found on the White Lupin genome portal
321 (<https://www.whitelupin.fr/>). The WL promoters (at least 1500 bp upstream start codon) of
322 these genes were cloned upstream the β -glucuronidase (GUS) sequence and introduced into
323 WL roots via *Agrobacterium rhizogenes*-mediated root transformation (Uhde-Stone *et al.*,
324 2005).

325 To characterize tissue specific expression, their expression pattern was first assessed into
326 secondary-order roots *i.e.* apex of cluster roots. CRs stained for GUS for each marker are
327 shown in Fig. 5, as well as cross sections produced in these lines. The *pLaWOL:GUS* line was
328 expressed in the stele of CR (Fig. 5A-B). Staining was not observed in the elongation zone
329 but was seen in the differentiation zone in the stele (Fig. S2A). A transverse section through
330 the differentiation zone shows GUS staining in stellar tissue along xylem axis and pericycle
331 cells facing the xylem poles (Fig. 5B). Staining in the stele disappears in the primordium
332 patterning zone and became restricted only to pericycle cells and the stele of the primordium.
333 (Fig. S2B). *pLaWOL:GUS* driven expression was observed in the stele of emerged rootlet
334 with a stronger staining in the meristematic zone where QC is expected to locate (Fig. S2C-E).
335 Expression of *pLaSCR1:GUS* in cluster roots matched previous reports (Sbabou *et al.*, 2010)
336 and was strongly specific of the endodermis of CR tip (Fig. 5C,D). Promoter expression was
337 also observed early on in rootlet primordia (Fig. S2F,G) and more specifically in the rootlet
338 meristematic zone after their emergence (Fig. S2H-I). Expression of the *pLaPEP:GUS*
339 construct was specific of cortical cells (Fig. 5E,F). Promoter is strongly expressed in the root
340 meristematic zone, and is not expressed in endodermis/cortex initial and the QC (Fig. 5E). A

341 transverse section in the beginning of elongation zone is shown in Fig. 5F showing the
342 specificity of the cortical expression. Expression tends to fade away in the elongation zone in
343 the shootward direction (not shown). Similar pattern for *pLaPEP:GUS* was observed in
344 primordium and emerged rootlet (Fig. S2K-O). Expression of the *pLaEXP7:GUS* construct
345 was absent from the very tip of the CR meristem and started at the onset of the elongation
346 zone (Fig. 5G). A cross section performed in the differentiation zone showed the specificity of
347 the epidermal expression (Fig. 5H). Staining was still present in the epidermal cells in the
348 primordium patterning zone (Fig. S2P) but was absent from primordium (Fig. S2Q) and
349 young rootlets (Fig. S2R,S). Expression resumes in older rootlets when elongation zone is
350 fully active (Fig. S2T). The study of the 4 selected marker genes suggested that 3 of them
351 could be used to further analysis during early rootlet primordium development (since *LaEXP7*
352 shows no expression). We therefore selected *pLaWOL:GUS*, *pLaSCR1:GUS* and
353 *pLaPEP:GUS* to provide a detailed description of rootlet developmental stages and tissue
354 differentiation.

355

356 *Tissue specific marker expression throughout rootlet primordia development*

357 The various stages of rootlet primordia development were studied from the early divisions up
358 to their emergence in order to determine when tissues differentiate and to provide a
359 developmental atlas of rootlet primordia development. We combined thick longitudinal cross
360 sections (Fig. 6) to provide stronger GUS staining together with thin radial cross sections
361 (Fig. 7) for better accuracy. The *pLaWOL:GUS* marker showed strong signal as early as stage
362 II (Fig. 6A) corresponding to 6 pericycle cells in P1/P2 right after the first periclinal division
363 (Fig. 7A). At later stages, the staining pattern becomes limited to a group of cells at the base
364 of the primordium that might be derived from P1 (Fig. 6B,C and Fig. 7B). From stage VI
365 onward, staining is clearly observed in elongated cells at the centre of the primordium (Fig.
366 6D and Fig. 7C). This pattern of expression remains similar up to after emergence
367 corresponding to the newly developed vasculature (Fig. 6E and Fig. 7D). The *pLaSCR1:GUS*
368 endodermal marker expression is first seen in 5 endodermal cells at stage II when these cells
369 appear to divide (Fig. 6F and Fig. 7E). At stage III and IV, staining is not only observed in E1
370 and E2 (Fig. 6G) but also in the overlaying cortical cells (Fig. 7F). At stage VI,
371 *pLaSCR1:GUS* expression starts to be restricted to two inner layers that are surrounding the
372 stele with a typical U-shaped profile (Fig. 6H). A group of cells abutting these two layers also
373 show weak GUS staining at the tip of the rootlet primordium (Fig. 7G). This expression
374 profile remains the same when the rootlet is about to emerge (Fig. 6I,J and Fig. 7H). Marker

375 line *pLaPEP:GUS* is not expressed in the first stages of rootlet development but is present in
376 the parental cluster root cortex (Fig. 6K-M and Fig. 7I). At stage V, a faded expression can be
377 observed in the tip of the primordium on thin sections (Fig. 7J). This faint expression profile
378 persists at stage VI (Fig. 7K). After emergence, staining is expressed in 3 to 4 cortical cell
379 layers at the edges of the primordium but is not expressed in younger cortical cell files
380 reminiscent of the expression pattern in cluster roots (Fig. 6N,O, Fig. 7L).

381

382 **Discussion**

383 Previous histological work has described cluster root development in white lupin, showing
384 that rootlets seemingly arise from divisions of pericycle cells facing xylem poles (Johnson *et*
385 *al.*, 1996; Hagström *et al.*, 2001; Watt and Evans, 2003). Here, we provide a detailed
386 anatomical study of rootlet development by taking advantage of molecular markers via
387 genetic transformation of white lupin roots (Uhde-Stone *et al.*, 2005). Our study reveals that
388 several tissues divide to participate to the formation of the primordium as shown by the cell
389 cycle marker *pAtCYCB1;1*. As in lateral root formation of most species, divisions in the
390 pericycle cells initiate the formation of new rootlets, but several rounds of divisions in
391 endodermal and cortical cells are also observed. These are reminiscent of lateral root
392 formation in other Legumes such as Medicago (Herrbach *et al.*, 2014) and other angiosperms
393 (Torres-Martínez *et al.*, 2019). It is not entirely clear to which extent these divisions in the
394 outer tissues contribute to the primordium itself or to a protective layer whose fate remains
395 undescribed in white lupin. The presence of more cell layers than in the model plant
396 *Arabidopsis*, where most of the real time description and cell lineage work has been
397 performed, suggests that different mechanisms may be involved. These mechanisms may not
398 be solely mechanical (stronger pressure, distinct cell wall remodelling processes) but may
399 also include active cell divisions to accommodate the passage of the rootlet primordium. The
400 existence of a temporary cap-like structure has been reported in other species (Torres-
401 Martínez *et al.*, 2019) and the numerous divisions in the endodermis seem to generate such
402 structure as can be seen on a Stage VI rootlet primordium (Fig. 1D). Further cell lineage
403 studies would be needed to clearly demonstrate to which extent these dividing cells from
404 outer layers (endodermis and cortex) participate to the primordium itself and hence to the
405 rootlet formation.

406 Within the rootlet primordium itself, cell division patterns (from the initiation in the pericycle
407 up to the establishment of an organized meristematic zone) is fairly similar to what has been
408 described in other plants and led us to separate its development into 8 stages, similarly to the

409 model plant *Arabidopsis* (Fig. 8). Although this staging could be seen as somehow artificial
410 due to the numerous extra division events in a multi-layered structure, we believe that it will
411 help comparing similar developmental stages between plant models, especially in the context
412 of transcriptomic analysis similar to the ones already described in *Arabidopsis* (Voß *et al.*,
413 2015). Interestingly, a meristematic structure is put into place during rootlet development and
414 several divisions occur at the final emergence stage VIII (Fig. 2E) but rootlet development
415 appears to be determinate at later stages (Watt and Evans, 1999). This implies that the
416 primordium meristematic structure, although apparently fully functional at the stages
417 described here, loses its division abilities and fully differentiates later on. Future work should
418 determine at which subsequent stages this switch operates.

419

420 **Acknowledgements**

421 This project has received funding from the European Research Council (ERC) under the
422 European Union's Horizon 2020 research and innovation program (Starting Grant
423 LUPINROOTS - grant agreement No 637420 to B.P.). C.G. is the recipient of a fellowship
424 from GAIA doctoral school of Montpellier University. We thank Carine Alcon (PHIV
425 platform) for the help in microscopy and access to imaging facility MRI, member of the
426 national infrastructure France-BioImaging.

427

References

- Abdolzadeh A, Wang X, Veneklaas EJ, Lambers H.** 2010. Effects of phosphorus supply on growth, phosphate concentration and cluster-root formation in three *Lupinus* species. *Ann Bot* **105**: 365-74
- Braum S, Helmke P.** 1995. White lupin utilizes soil phosphorus that is unavailable to soybean. *Plant Soil* **176**: 95-100
- Byrne JM, Pesacreta TC, Fox JA.** 1977. Development and structure of the vascular connection between the primary and secondary roots of *Glycine max* (L.) Merr. *Am J Bot* **64**: 946-959
- Cheng L, Bucciarelli B, Shen J, Allan D, Vance CP.** 2011. Update on lupin cluster roots. Update on white lupin cluster root acclimation to phosphorus deficiency. *Plant Physiol* **156**: 1025-32
- Colón-Carmona A, You R, Haimovitch-Gal T, Doerner P.** 1999. Technical advance: spatio-temporal analysis of mitotic activity with a labile cyclin-GUS fusion protein. *Plant J* **20**: 503-8

- Cu ST, Hutson J, Schuller KA.** 2005. Mixed culture of wheat (*Triticum aestivum* L.) with white lupin (*Lupinus albus* L.) improves the growth and phosphorus nutrition of the wheat Plant and soil **272**: 143-151
- Delaux PM, Varala K, Edger PP, Coruzzi GM, Pires JC, Ané JM.** 2014. Comparative phylogenomics uncovers the impact of symbiotic associations on host genome evolution. PLoS Genet **10**: e1004487
- Dinkelaker B, Hengeler C, Marschner H.** 1995. Distribution and function of proteoid roots and other root clusters Botanica Acta (Germany) **108**: 183-200
- Dinkelaker B, Römheld V, Marschner H.** 1989. Citric acid excretion and precipitation of calcium citrate in the rhizosphere of white lupin (*Lupinus albus* L.). Plant Cell Environ **12**: 285-92
- Gallardo C, Hufnagel B, Casset C, Alcon C, Garcia F, Divol F, Marquès L, Doumas P, Péret B.** 2019. Anatomical and hormonal description of rootlet primordium development along white lupin cluster root. Physiol Plant **165**: 4-16
- Goh T, Toyokura K, Wells DM, Swarup K, Yamamoto M, Mimura T, Weijers D, Fukaki H, Laplaze L, Bennett MJ, Guyomarc'h S.** 2016. Quiescent center initiation in the Arabidopsis lateral root primordia is dependent on the SCARECROW transcription factor. Development
- Hagström J, James WM, Skene KR.** 2001. A comparison of structure, development and function in cluster roots of *Lupinus albus* L. under phosphate and iron stress Plant and Soil **232**: 81-90
- Herrbach V, Remblière C, Gough C, Bensmihen S.** 2014. Lateral root formation and patterning in *Medicago truncatula*. J Plant Physiol **171**: 301-10
- Hochholdinger F, Park WJ, Sauer M, Woll K.** 2004. From weeds to crops: genetic analysis of root development in cereals. Trends Plant Sci **9**: 42-8
- Hufnagel B, Marques A, Soriano A, Marquès L, Divol F, Doumas P, Sallet E, Mancinotti D, Carrere S, Marande W, Arribat S, Keller J, Huneau C, Blein T, Aimé D, Laguerre M, Taylor J, Schubert V, Nelson M, Geu-Flores F, Crespi M, Gallardo K, Delaux PM, Salse J, Bergès H, Guyot R, Gouzy J, Péret B.** 2020. High-quality genome sequence of white lupin provides insight into soil exploration and seed quality. Nat Commun **11**: 492
- Johnson JF, Vance CP, Allan DL.** 1996. Phosphorus deficiency in *Lupinus albus*. Altered lateral root development and enhanced expression of phosphoenolpyruvate carboxylase. Plant Physiol **112**: 31-41

- Lambers H, Cramer MD, Shane MW, Wouterlood M, Poot P, Vneklaas EJ.** 2003. Structure and functioning of cluster roots and plant responses to phosphate deficiency Plant and Soil **248**: IX-XIX
- Lambers H, Martinoia E, Renton M.** 2015. Plant adaptations to severely phosphorus-impooverished soils. Curr Opin Plant Biol **25**: 23-31
- Lamont BB .** 2003. Structure, ecology and physiology of root clusters--a review Plant and Soil **248**: 1-19
- Laskowski MJ, Williams ME, Nusbaum HC, Sussex IM.** 1995. Formation of lateral root meristems is a two-stage process. Development **121**: 3303-10
- Lemoine F, Correia D, Lefort V, Doppelt-Azeroual O, Mareuil F, Cohen-Boulakia S, Gascuel O.** 2019. NGPhylogeny.fr: new generation phylogenetic services for non-specialists. Nucleic Acids Res **47**: W260-W265
- Letunic I, Bork P.** 2019. Interactive Tree Of Life (iTOL) v4: recent updates and new developments. Nucleic Acids Res **47**: W256-W259
- Li H, Shen J, Zhang F, Marschner P, Cawthray G, Rengel Z.** 2010. Phosphorus uptake and rhizosphere properties of intercropped and monocropped maize, faba bean, and white lupin in acidic soil. Biol. Fertil. Soils **46**: 79-91
- Lynch J, Brown M.** 2001. Topsoil foraging – an architectural adaptation of plants to low phosphorus availability Plant Soil **237**: 225-237
- Maherali H, Oberle B, Stevens PF, Cornwell WK, McGlenn DJ.** 2016. Mutualism Persistence and Abandonment during the Evolution of the Mycorrhizal Symbiosis. Am Nat **188**: E113-E125
- Malamy JE, Benfey PN.** 1997. Organization and cell differentiation in lateral roots of Arabidopsis thaliana. Development **124**: 33-44
- Marquès-Bueno MDM, Morao AK, Cayrel A, Platre MP, Barberon M, Caillieux E, Colot V, Jaillais Y, Roudier F, Vert G.** 2016. A versatile Multisite Gateway-compatible promoter and transgenic line collection for cell type-specific functional genomics in Arabidopsis. Plant J **85**: 320-333
- Massonneau A, Langlade N, Léon S, Smutny J, Vogt E, Neumann G, Martinoia E.** 2001. Metabolic changes associated with cluster root development in white lupin (*Lupinus albus* L.): relationship between organic acid excretion, sucrose metabolism and energy status. Planta **213**: 534-42
- Neumann G, Martinoia E.** 2002. Cluster roots--an underground adaptation for survival in extreme environments. Trends Plant Sci **7**: 162-7

- Oba H, Tawaray K, Wagatsuma T.** 2001. Arbuscular mycorrhizal colonization in *Lupinus* and related genera. *Soil Sci. Plant Nutr.* **47**: 685-694
- Op den Camp R, De Mita S, Lillo A, Cao Q, Limpens E, Bisseling T, Geurts R.** 2011. A phylogenetic strategy based on a legume-specific whole genome duplication yields symbiotic cytokinin type-A Response Regulators. *Plant Physiol* **157**: 2013-22
- Orman-Ligeza B, Parizot B, Gantet PP, Beeckman T, Bennett MJ, Draye X.** 2013. Post-embryonic root organogenesis in cereals: branching out from model plants. *Trends Plant Sci* **18**: 459-67
- Sas L, Rengel Z, Tang C.** 2001. Excess cation uptake, and extrusion of protons and organic acid anions by *Lupinus albus* under phosphorus deficiency. *Plant Sci* **160**: 1191-1198
- Sbabou L, Bucciarelli B, Miller S, Liu J, Berhada F, Filali-Maltouf A, Allan D, Vance C.** 2010. Molecular analysis of SCARECROW genes expressed in white lupin cluster roots. *J Exp Bot* **61**: 1351-63
- Sevin-Pujol A, Sicard M, Rosenberg C, Auriac MC, Lepage A, Niebel A, Gough C, Bensmihen S.** 2017. Development of a GAL4-VP16/UAS trans-activation system for tissue specific expression in *Medicago truncatula*. *PLoS One* **12**: e0188923
- Skene KR.** 1998. Cluster roots: some ecological considerations *Journal of Ecology* **86**: 1060-1064
- Torres-Martínez HH, Rodríguez-Alonso G, Shishkova S, Dubrovsky JG.** 2019. Lateral Root Primordium Morphogenesis in Angiosperms. *Front Plant Sci* **10**: 206
- Trinh C, Laplaze L, Guyomarc'h S.** 2018. Lateral Root Formation: Building a Meristem *de novo* *Annual Plant Reviews Online* **1**:
- Uhde-Stone C, Gilbert G, Johnson JM-F, Litjens R, Zinn KE, Temple SJ, Vance CP, Allan DL.** 2003. Acclimation of white lupin to phosphorus deficiency involves enhanced expression of genes related to organic acid metabolism *Plant and Soil* 99-116
- Uhde-Stone C, Liu J, Zinn KE, Allan DL, Vance CP.** 2005. Transgenic proteoid roots of white lupin: a vehicle for characterizing and silencing root genes involved in adaptation to P stress. *Plant J* **44**: 840-53
- Vorster P, Jooste J.** 1986. Potassium and phosphate absorption by excised ordinary and proteoid roots of the Proteaceae. *South African J. Bot.* **52**: 277-281
- Voß U, Wilson MH, Kenobi K, Gould PD, Robertson FC, Peer WA, Lucas M, Swarup K, Casimiro I, Holman TJ, Wells DM, Péret B, Goh T, Fukaki H, Hodgman TC, Laplaze L, Halliday KJ, Ljung K, Murphy AS, Hall AJ, Webb AA, Bennett MJ.** 2015. The circadian clock rephases during lateral root organ initiation in *Arabidopsis*

thaliana. Nat Commun **6**: 7641

Watt M, Evans JR. 1999. Linking development and determinacy with organic acid efflux from proteoid roots of white lupin grown with low phosphorus and ambient or elevated atmospheric CO₂ concentration Plant Physiol **120**: 705-16

Watt M, Evans JR. 1999. Linking development and determinacy with organic acid efflux from proteoid roots of white lupin grown with low phosphorus and ambient or elevated atmospheric CO₂ concentration Plant Physiology **120**: 705-716

Watt M, Evans JR. 2003. Phosphorus acquisition from soil by white lupin (*Lupinus albus* L.) and soybean (*Glycine max* L.), species with contrasting root development Plant and Soil 271-283

Tables

Table S1. List of gene names and ID numbers, sequence of primers used for cloning.

Figure legends

Fig. 1. Histological description of the 8 stages of rootlet primordium formation.

(A) Whole root system of a 21-day old white lupin in phosphate deficiency conditions harbouring numerous cluster roots. (B) One cluster root harbouring numerous rootlets. (C) Nuclear staining (DAPI) of rootlet primordium during the emergence stage. (D) Longitudinal sections of a cluster root depicting all developmental stages of rootlet development (ruthenium red stained). Last image (StVII) is a cross section. St0: Stage 0. Parental tissues before visible events. StIa: Stage Ia. First asymmetric division in the pericycle. StIb: Stage Ib. First periclinal division in the pericycle and first anticlinal division in the endodermis. StII: Stage II. Formation of a flattened four-layered primordium: two pericycle layers and two endodermal layers. StIII: Stage III. Several rounds of extra anticlinal divisions in the endodermis and first cortical divisions. StIV: Stage IV. Divisions rate increase and start to shape a dome. StV: Stage V. The dome shape is now well established and the rootlet primordium passes through the cortical layers. StVI: Stage VI. The primordium is now half-way through the cortical layers. StVII: Stage VII. The rootlet primordium is about to emerge from the maternal root. p: pericycle, e: endodermis, c: cortex. Arrows pinpoint key division planes. Scale bars: 1 cm (A), 1mm (B), 200 μ m (C), 50 μ m (D).

Fig. 2. Cell divisions during rootlet formation marked by the Arabidopsis *pAtCYCB1;1:GUS* marker. (A-E) Thin cross sections of hairy root transformed cluster roots

expressing the *pAtCYCB1;1:GUS* marker of the G2/M transition of the cell cycle. (A) Stage 0: one pericycle cell in front of each xylem pole expresses the marker. (B) Close-up view of the earliest observable event of rootlet initiation depicting one cell preparing to divide. (C) Stage II: active divisions in the pericycle and endodermis. (D) Stage IV: numerous divisions occur in the pericycle, endodermis and cortex. (E) Stage VII: just prior to emergence, numerous divisions are seen in what appears to be a fully functional and organized meristem. Scale bars are 100 μm (A) and 50 μm (B-E).

Fig. 3. Maximum likelihood phylogenetic tree of white lupin orthologs and Arabidopsis gene markers. The trees were constructed using the phylogeny tool from NGPhylogeny.fr (<https://ngphylogeny.fr/>). Branches lengths are displayed. The orthologs selected to further experiments are highlighted. Analyses were performed using protein sequences extracted from white lupin genome (<https://www.whitelupin.fr/>) and from public database TAIR (<https://www.arabidopsis.org>) belonging to the model plant *Arabidopsis thaliana* and to the following Legume species: *Medicago truncatula*, *Cicer arietinum*, *Lupinus angustifolius* and *Glycine max*.

Fig. 4. Candidate marker gene expression across rootlet development. (A) Data coming from transcriptomic temporal dataset of 8 developmental stages of rootlet formation as described in (Hufnagel *et al.*, 2020). (B-E) Expression profile of white lupin ortholog genes to Arabidopsis tissue specific markers. Red lines indicate genes for which promoters were cloned for further studies. Data are mean \pm SD of four biological replicates coming each from ten cluster roots sampled across 5 lupin plants (n=10).

Fig. 5. Expression profiles of four white lupin promoters in the second order root. Promoter profiles shown are: *pLaWOL* (A, B), *pLaSCR1* (C, D), *pLaPEP* (E, F), *pLaEXP7* (G, H). Images are longitudinal sections in the meristematic and elongation zones of the tip of the cluster root (A, C, E, G). Cross sections were performed through different cluster root zones: the meristematic zone (D), the elongation zone (F), the differentiation zone (B, H). Scale bars are 100 μm .

Fig. 6. Expression of tissue-specific molecular markers during rootlet primordium development on thick longitudinal sections through cluster roots. Images are 80 μm thick sections showing GUS activity in 3 marker lines. (A-E) *pLaWOL:GUS*. (A) StII. Staining is

seen the pericycle. (B, C) StIII, StIV. Staining is observed in the stele-derived tissues. (D,E) StVII, StVIII. Staining is observed in central tissues at the core of the rootlet primordium. (F,J) *pLaSCRI:GUS*. (F,G) StII, StIII. Staining is observed only in the endodermis. (H-J) St VI, VII, VIII. Staining appear to be expressed in layers surrounding the stele. (K-O) *pLaPEP:GUS*. (K,L) StII, StIII. Staining is seen in the cortex of the cluster root but is not expressed in the primordium. (M) StVI. Staining appears in the cortical cells overlaying the primordium. (N,O). StVII, StVIII. Staining is observed in both sides of the primordium but the region at the tip is unstained. Scale bar: 50 μm (A-O).

Fig. 7. Expression of tissue-specific molecular markers during rootlet primordium development on thin longitudinal sections through cluster roots. Images are 5 μm thin sections showing GUS activity in 3 marker lines. (A-D) *pLaWOL:GUS*. (A) StII. Lupin promoter is specifically expressed in pericycle cell opposite xylem pole, 6 of which seem to be dividing. (B). StV. Staining is apparent in few cells at the base of the primordium. (C, D) StVI, StVIII. Staining is observed in elongated cells found at the core of the primordium. (E-H) *pLaSCRI:GUS*. (E) StII. Staining appear specifically in 6 endodermal cells that appear to be dividing. (F) StIV. GUS staining appear in E1/E2 endodermal layers and cortical cells. (G, H) StVI, StVII. Staining is restricted to two layers around central stele and a group of cells at the tip of the rootlet (asterisk). (I-L) *pLaPEP:GUS*. (I) StIII. GUS staining is difficult to observe at this stage. (J, K) StV, StVI. Weak staining in cortical cells at the tip of rootlet. (L). GUS staining is observed in tissues at the edges of the primordium. Scale bar: 50 μm (A-L).

Fig. 8. The 8 stages of rootlet development in white lupin. Scheme based on longitudinal sections of white lupin rootlets. Colours indicate putative cell tissues in the growing rootlet primordium from stage I to stage VII. Stage VIII (not represented) would be similar to Stage VII but when the primordium crosses the final layer to reach the rhizosphere. St0: Stage 0, prior to visible divisions, only molecular markers such as *pAtCYCB1;1* can reveal that a site for rootlet formation has been activated. St1a: Stage 1a, first two asymmetrical divisions are seen in pericycle. St1b: Stage 1b, periclinal divisions in pericycle give rise to two layers, P₁ and P₂. StII: Stage II, periclinal divisions in endodermis give rise to two layers E₁ and E₂. StIII: Stage III, divisions in adjacent cortical cells. StIV: Stage IV, rootlet patterning and tissue differentiation. StV: Stage V, elongation of vascular cells. StVI: Stage VI, differentiation of tissue layers inside rootlet primordium. StVII: Stage VI, further growth of

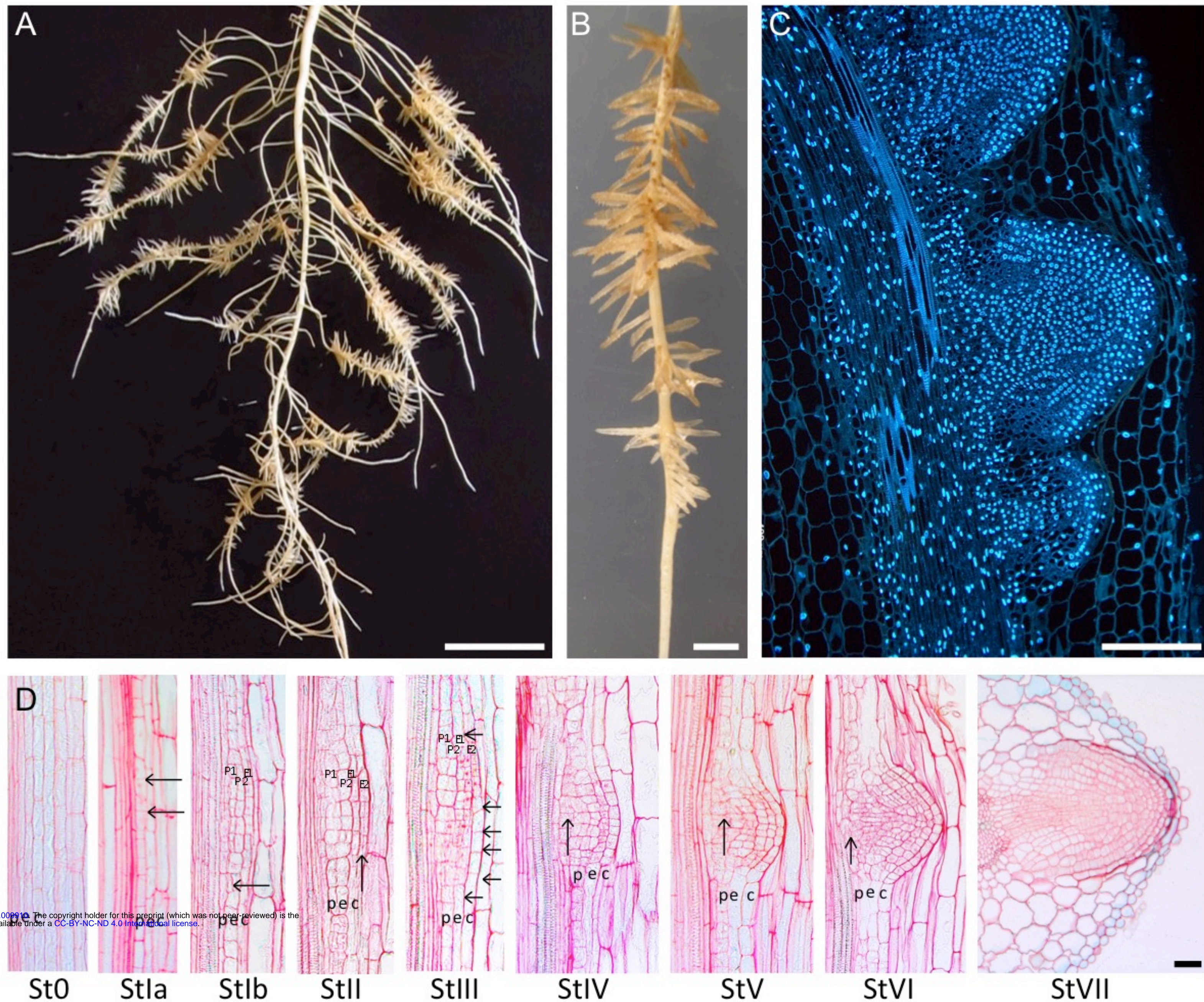
the primordium until it reaches the epidermal layer and prior to emergence (StVIII: Stage VIII).

Supplementary data

Fig. S1. Expression profile of the *pAtCYCB1;1:GUS* marker in white lupin cluster root is associated with sites with active cell divisions. (A) Cluster root tip shows typical spotted expression of dividing cells in the meristematic region. (B) In the differentiation zone, sites of rootlet formation show expression of the marker at early initiation stages. (C) Later on, cell divisions in the rootlet primordium are also seen. (D) Cell divisions can be seen in the active rootlet primordium upon their emergence. Bars are 350 μ m.

Fig. S2. Expression profiles of four white lupin promoters in cluster roots. Promoters profiles shown are: *pLaWOL:GUS* (A-E), *pLaSCRI:GUS* (F-J), *pLaPEP:GUS* (K-O) and *pLaEXP7:GUS* (P-T). Whole-mount view of early differentiation zone (A, F, K and P), late differentiation zone with late stages rootlet primordia (B, G, L and Q), rootlet emergence (C, H, M and R), rootlet midgrowth stage (D, I, N and S) and fully grown rootlets (E, J, O and T). Scale bars are 150 μ m (column 1-4), 500 μ m (column 5).

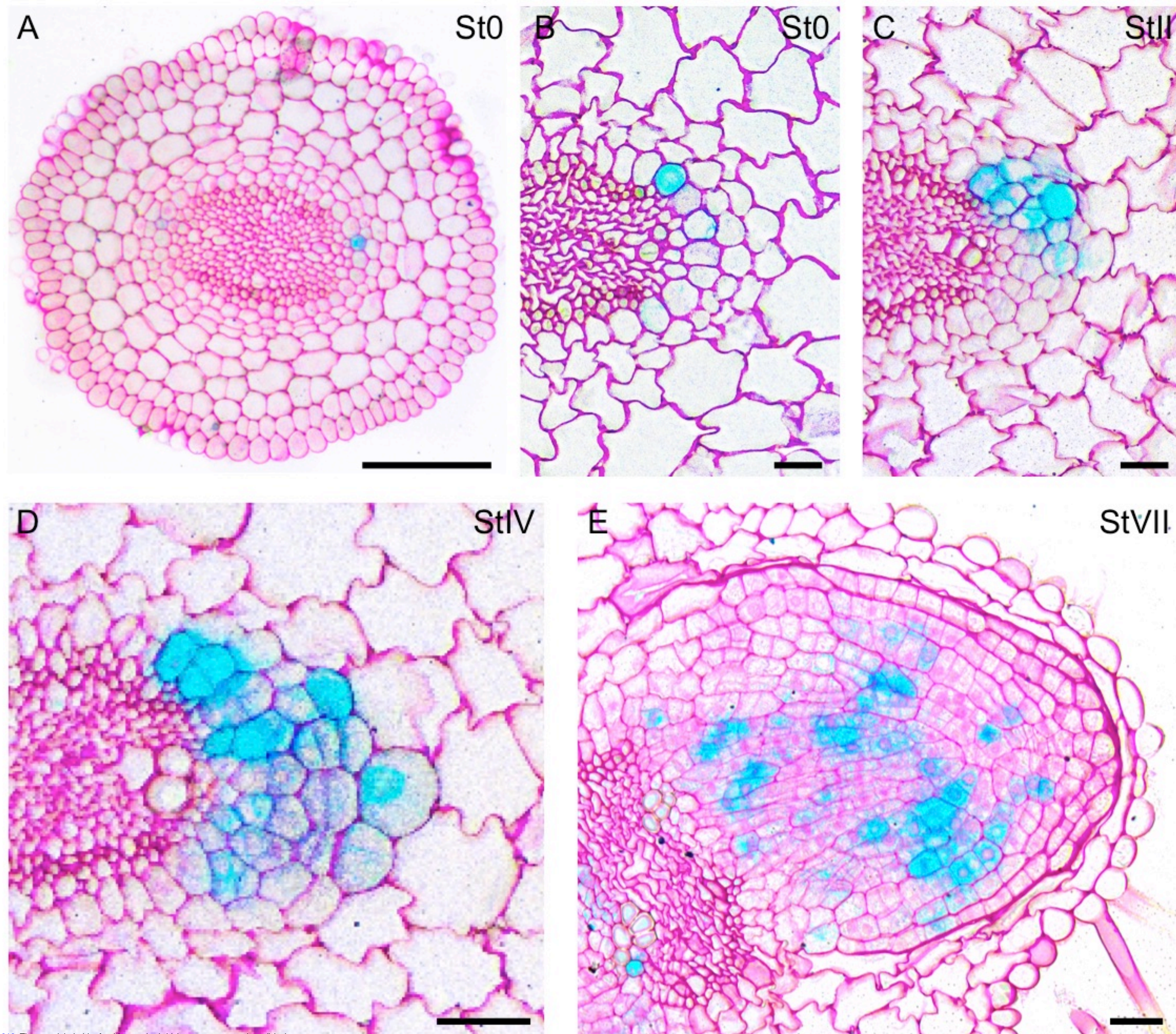
Figure 1



bioRxiv preprint doi: <https://doi.org/10.1101/2020.03.26.009191>; this version posted March 26, 2020. The copyright holder for this preprint (which was not certified by peer review) is the author/funder. It is made available under aCC-BY-NC-ND 4.0 International license.

Fig. 1. Histological description of the 8 stages of rootlet primordium formation. (A) Whole root system of a 21-day old white lupin in phosphate deficiency conditions harbouring numerous cluster roots. (B) One cluster root harbouring numerous rootlets. (C) Nuclear staining (DAPI) of rootlet primordium during the emergence stage. (D) Longitudinal sections of a cluster root depicting all developmental stages of rootlet development (ruthenium red stained). Last image (StVII) is a cross section. St0: Stage 0. Parental tissues before visible events. StIa: Stage Ia. First asymmetric division in the pericycle. StIb: Stage Ib. First periclinal division in the pericycle and first anticlinal division in the endodermis. StII: Stage II. Formation of a flattened four-layered primordium: two pericycle layers and two endodermal layers. StIII: Stage III. Several rounds of extra anticlinal divisions in the endodermis and first cortical divisions. StIV: Stage IV. Divisions rate increase and start to shape a dome. StV: Stage V. The dome shape is now well established and the rootlet primordium passes through the cortical layers. StVI: Stage VI. The primordium is now half-way through the cortical layers. StVII: Stage VII. The rootlet primordium is about to emerge from the maternal root. p: pericycle, e: endodermis, c: cortex. Arrows pinpoint key division planes. Scale bars: 1 cm (A), 1mm (B), 200 μ m (C), 50 μ m (D).

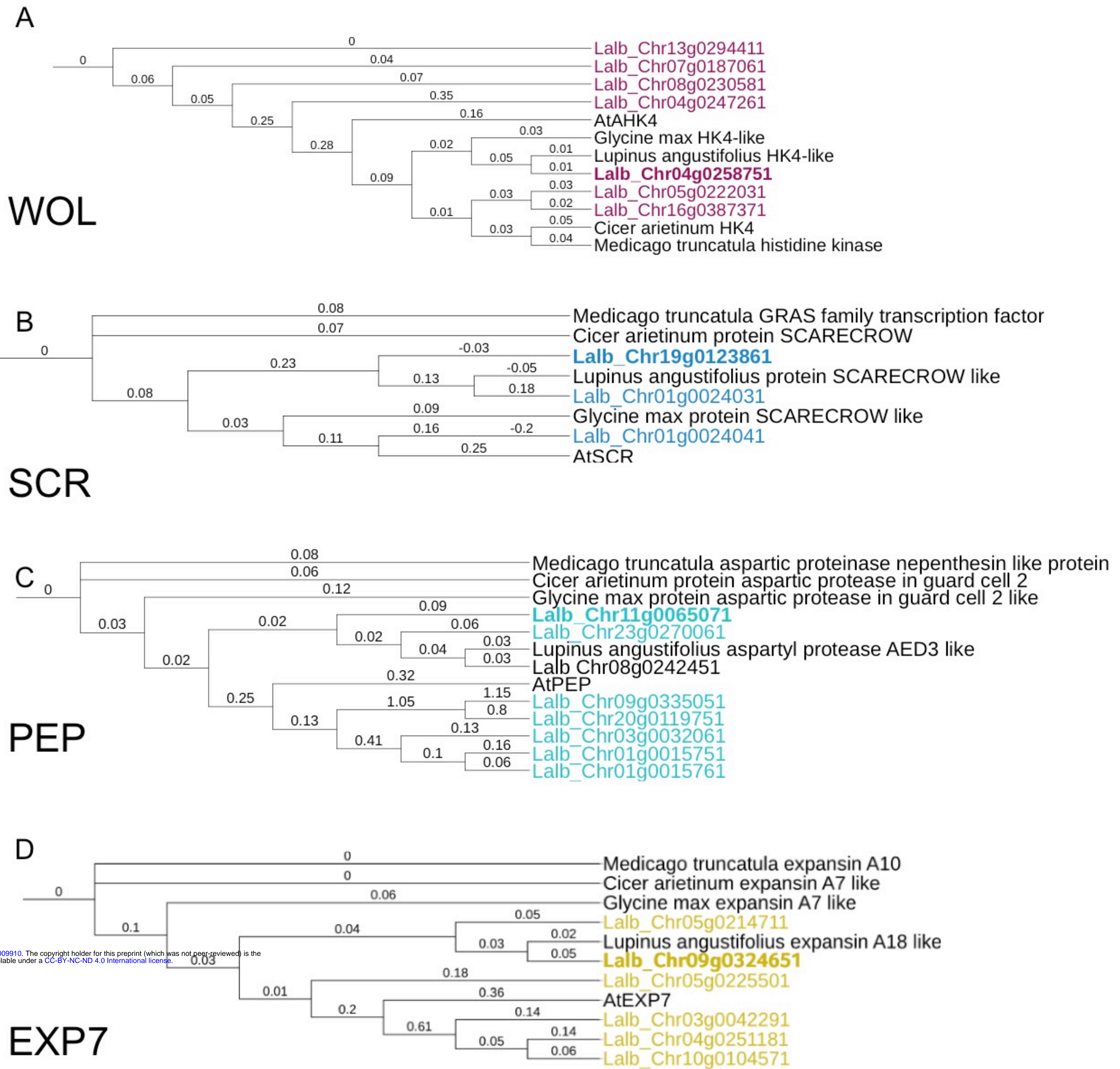
Figure 2



bioRxiv preprint doi: <https://doi.org/10.1101/2020.03.26.009910>; this version posted March 26, 2020. The copyright holder for this preprint (which was not peer-reviewed) is the author/funder. It is made available under aCC-BY-NC-ND 4.0 International license.

Fig. 2. Cell divisions during rootlet formation marked by the *Arabidopsis pAtCYCB1;1:GUS* marker. (A-E) Thin cross sections of hairy root transformed cluster roots expressing the *pAtCYCB1;1:GUS* marker of the G2/M transition of the cell cycle. (A) Stage 0: one pericycle cell in front of each xylem pole expresses the marker. (B) Close-up view of the earliest observable event of rootlet initiation depicting one cell preparing to divide. (C) Stage II: active divisions in the pericycle and endodermis. (D) Stage IV: numerous divisions occur in the pericycle, endodermis and cortex. (E) Stage VII: just prior to emergence, numerous divisions are seen in what appears to be a fully functional and organized meristem. Scale bars are 100 μm (A) and 50 μm (B-E).

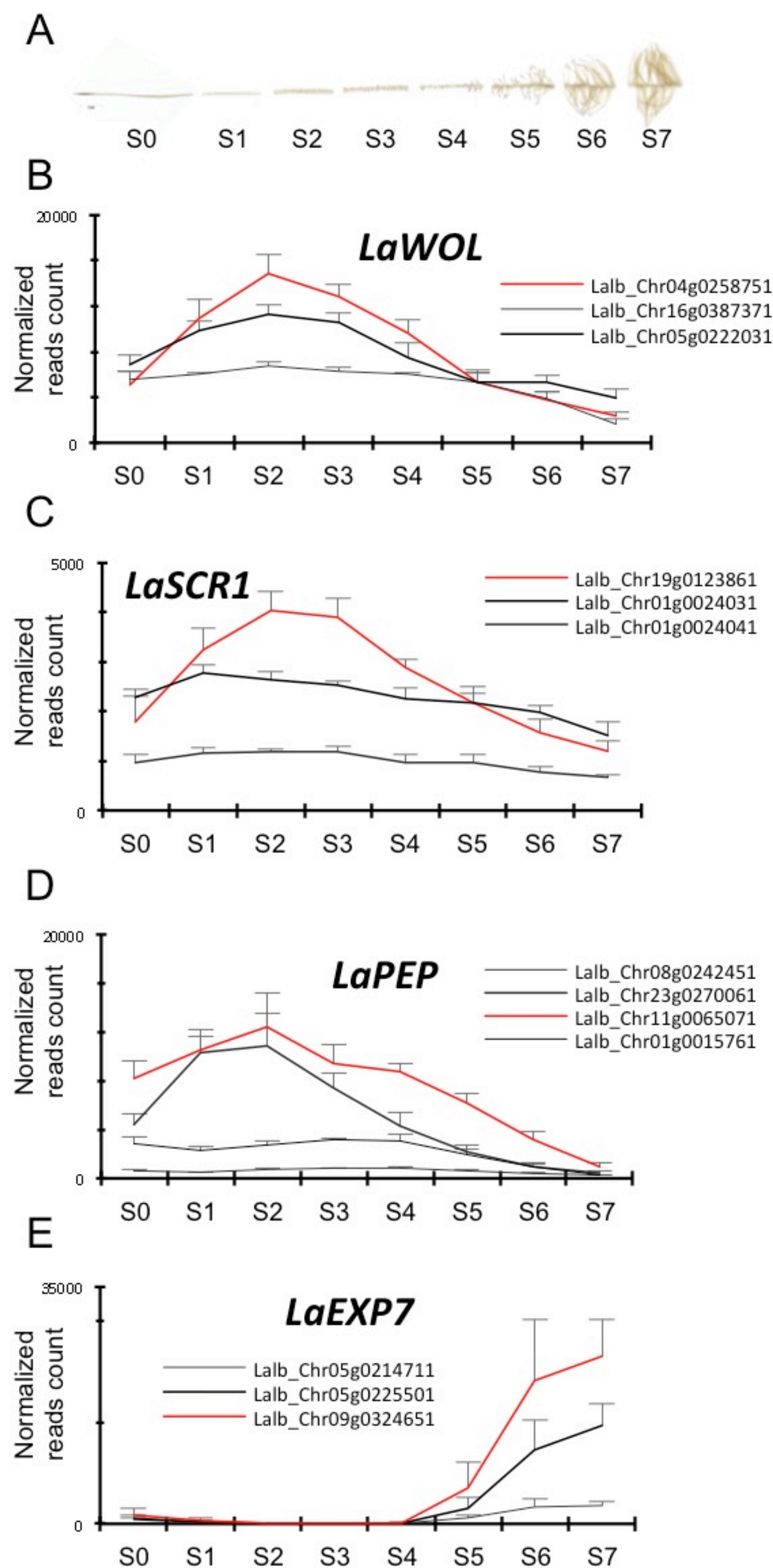
Figure 3



bioRxiv preprint doi: <https://doi.org/10.1101/2020.03.26.009910>; this version posted March 26, 2020. The copyright holder for this preprint (which was not certified by peer review) is the author/funder. It is made available under aCC-BY-NC-ND 4.0 International license.

Fig. 3. Maximum likelihood phylogenetic tree of white lupin orthologs and Arabidopsis gene markers. The trees were constructed using the phylogeny tool from NGPhylogeny.fr (<https://ngphylogeny.fr/>). Branches lengths are displayed. The orthologs selected to further experiments are highlighted. Analyses were performed using protein sequences extracted from white lupin genome (<https://www.whitelupin.fr/>) and from public database TAIR (<https://www.arabidopsis.org>) belonging to the model plant *Arabidopsis thaliana* and to the following Legume species: *Medicago truncatula*, *Cicer arietinum*, *Lupinus angustifolius* and *Glycine max*.

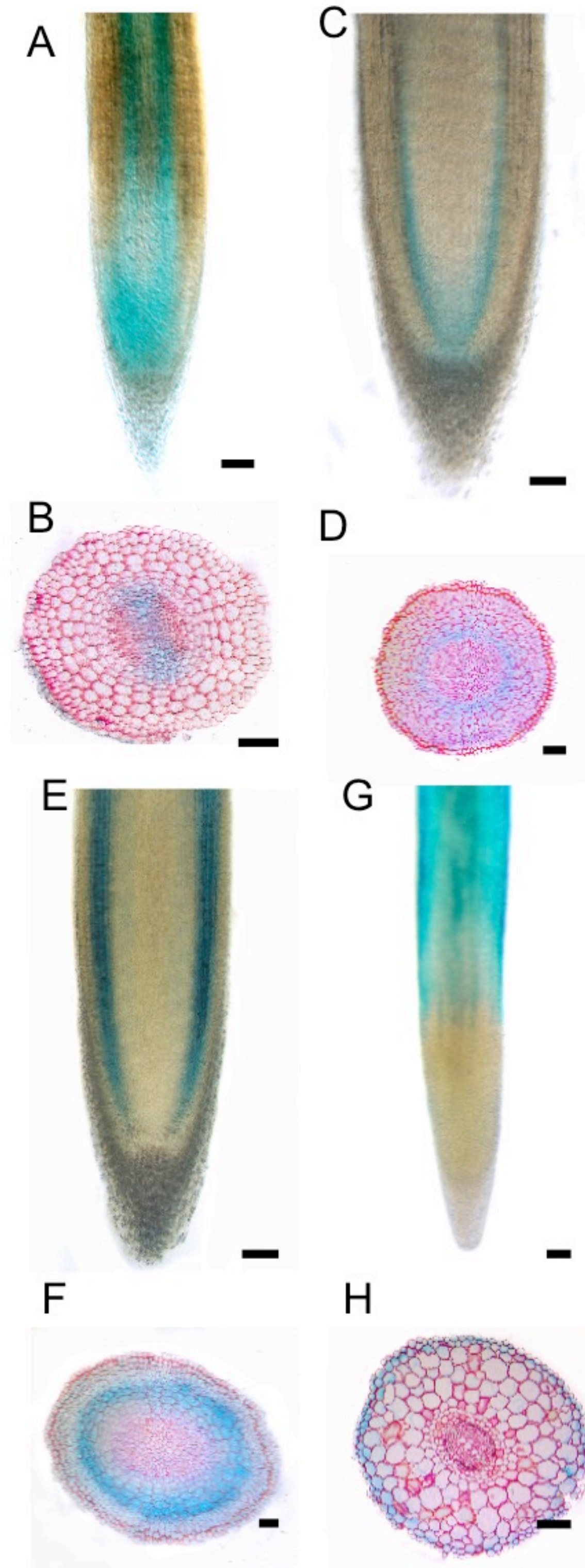
Figure 4



bioRxiv preprint doi: <https://doi.org/10.1101/2020.03.26.009910>; this version posted March 26, 2020. The copyright holder for this preprint (which was not peer-reviewed) is the author/funder. It is made available under aCC-BY-NC-ND 4.0 International license.

Fig. 4. Candidate marker gene expression across rootlet development. (A) Data coming from transcriptomic temporal dataset of 8 developmental stages of rootlet formation as described in (Hufnagel *et al.*, 2020). (B-E) Expression profile of white lupin ortholog genes to Arabidopsis tissue specific markers. Red lines indicate genes for which promoters were cloned for further studies. Data are mean \pm SD of four biological replicates coming each from ten cluster roots sampled across 5 lupin plants (n=10).

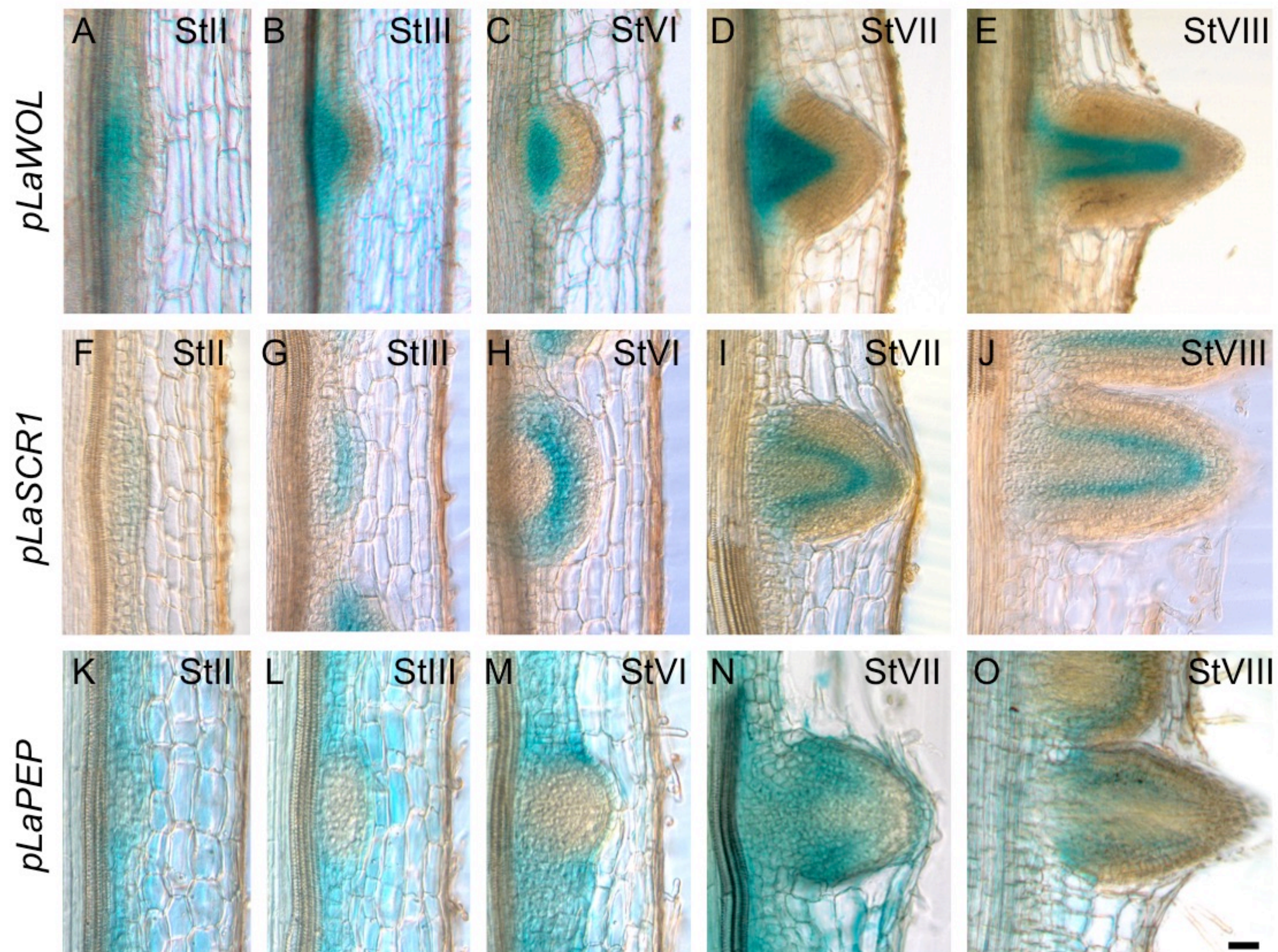
Figure 5



bioRxiv preprint doi: <https://doi.org/10.1101/2020.03.26.009910>; this version posted March 26, 2020. The copyright holder for this preprint (which was not peer-reviewed) is the author/funder. It is made available under aCC-BY-NC-ND 4.0 International license.

Fig. 5. Expression profiles of four white lupin promoters in the second order root. Promoter profiles shown are: *pLaWOL* (A, B), *pLaSCR1* (C, D), *pLaPEP* (E, F), *pLaEXP7* (G, H). Images are longitudinal sections in the meristematic and elongation zones of the tip of the cluster root (A, C, E, G). Cross sections were performed through different cluster root zones: the meristematic zone (D), the elongation zone (F), the differentiation zone (B, H). Scale bars are 100 μ m.

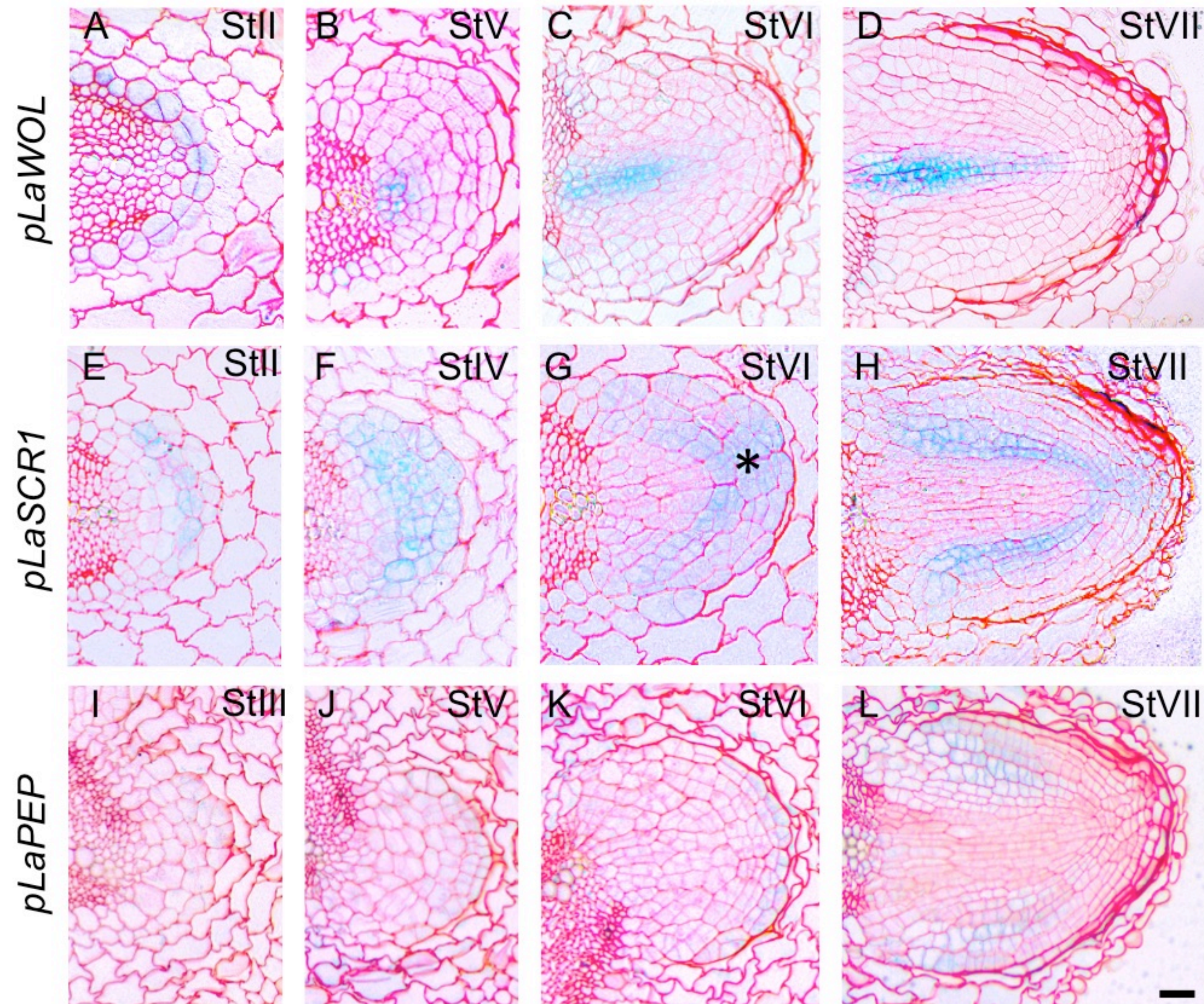
Figure 6



bioRxiv preprint doi: <https://doi.org/10.1101/2020.03.26.009910>; this version posted March 26, 2020. The copyright holder for this preprint (which was not peer-reviewed) is the author/funder. It is made available under aCC-BY-NC-ND 4.0 International license.

Fig. 6. Expression of tissue-specific molecular markers during rootlet primordium development on thick longitudinal sections through cluster roots. Images are 80 μm thick sections showing GUS activity in 3 marker lines. (A-E) *pLaWOL:GUS*. (A) StII. Staining is seen the pericycle. (B, C) StIII, StIV. Staining is observed in the stele-derived tissues. (D,E) StVII, StVIII. Staining is observed in central tissues at the core of the rootlet primordium. (F,J) *pLaSCR1:GUS*. (F,G) StII, StIII. Staining is observed only in the endodermis. (H-J) St VI, VII, VIII. Staining appear to be expressed in layers surrounding the stele. (K-O) *pLaPEP:GUS*. (K,L) StII, StIII. Staining is seen in the cortex of the cluster root but is not expressed in the primordium. (M) StVI. Staining appears in the cortical cells overlaying the primordium. (N,O). StVII, StVIII. Staining is observed in both sides of the primordium but the region at the tip is unstained. Scale bar: 50 μm (A-O).

Figure 7



bioRxiv preprint doi: <https://doi.org/10.1101/2020.03.26.009910>; this version posted March 26, 2020. The copyright holder for this preprint (which was not peer-reviewed) is the author/funder. It is made available under aCC-BY-NC-ND 4.0 International license.

Fig. 7. Expression of tissue-specific molecular markers during rootlet primordium development on thin longitudinal sections through cluster roots. Images are 5 μm thin sections showing GUS activity in 3 marker lines. (A-D) *pLaWOL:GUS*. (A) StII. Lupin promoter is specifically expressed in pericycle cell opposite xylem pole, 6 of which seem to be dividing. (B). StV. Staining is apparent in few cells at the base of the primordium. (C, D) StVI, StVIII. Staining is observed in elongated cells found at the core of the primordium. (E-H) *pLaSCR1:GUS*. (E) StII. Staining appear specifically in 6 endodermal cells that appear to be dividing. (F) StIV. GUS staining appear in E1/E2 endodermal layers and cortical cells. (G, H) StVI, StVII. Staining is restricted to two layers around central stele and a group of cells at the tip of the rootlet (asterisk). (I-L) *pLaPEP:GUS*. (I) StIII. GUS staining is difficult to observe at this stage. (J, K) StV, StVI. Weak staining in cortical cells at the tip of rootlet. (L). GUS staining is observed in tissues at the edges of the primordium. Scale bar: 50 μm (A-L).

Figure 8

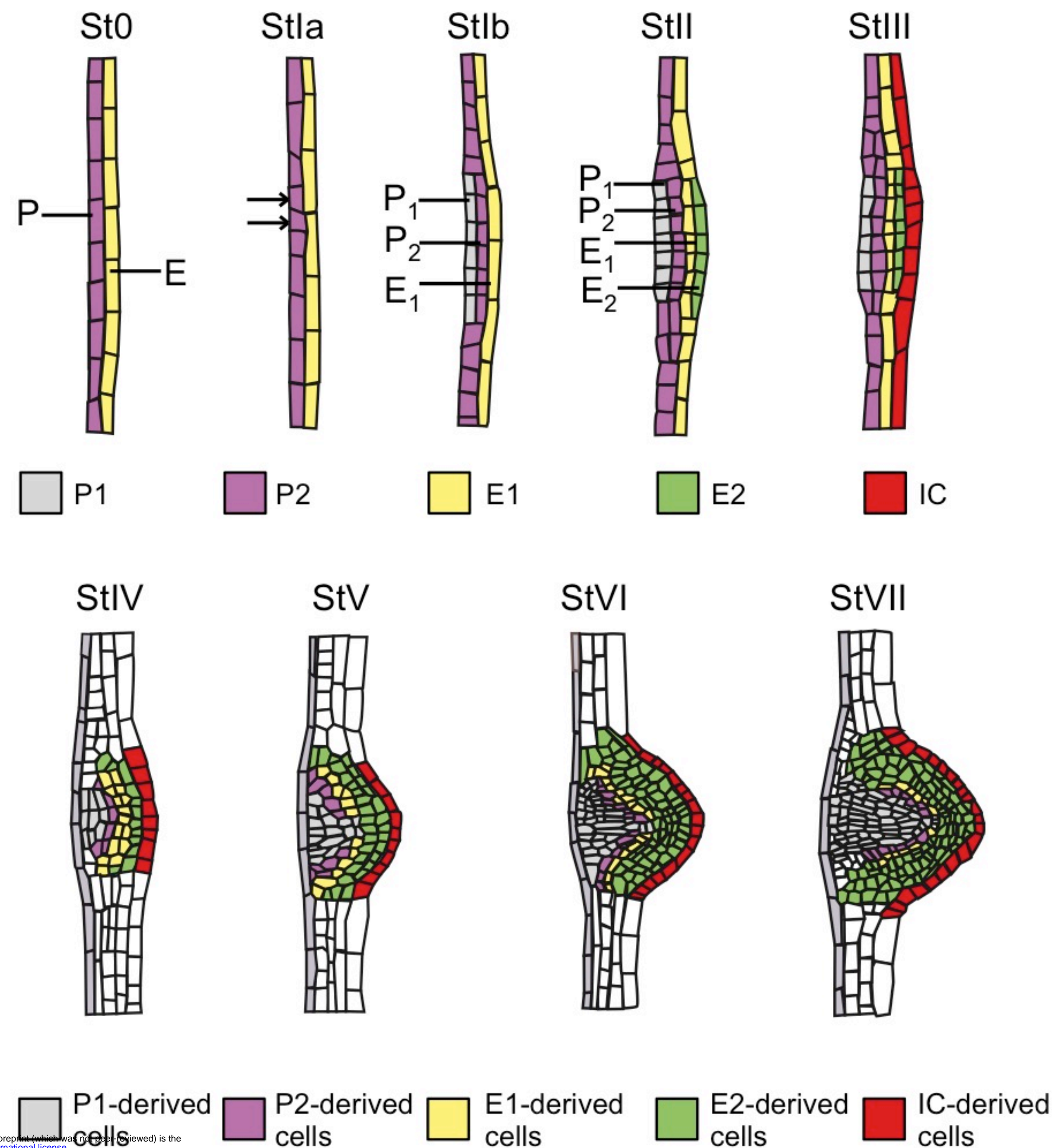


Fig. 8. The 8 stages of rootlet development in white lupin. Scheme based on longitudinal sections of white lupin rootlets. Colours indicate putative cell tissues in the growing rootlet primordium from stage I to stage VII. Stage VIII (not represented) would be similar to Stage VII but when the primordium crosses the final layer to reach the rhizosphere. St0: Stage 0, prior to visible divisions, only molecular markers such as *pAtCYCB1;1* can reveal that a site for rootlet formation has been activated. StIa: Stage 1a, first two asymmetrical divisions are seen in pericycle. StIb: Stage 1b, periclinal divisions in pericycle give rise to two layers, P₁ and P₂. StII: Stage II, periclinal divisions in endodermis give rise to two layers E₁ and E₂. StIII: Stage III, divisions in adjacent cortical cells. StIV: Stage IV, rootlet patterning and tissue differentiation. StV: Stage V, elongation of vascular cells. StVI: Stage VI, differentiation of tissue layers inside rootlet primordium. StVII: Stage VI, further growth of the primordium until it reaches the epidermal layer and prior to emergence (StVIII: Stage VIII).